Formation of the BMP Activity Gradient in the *Drosophila* Embryo

Claudia Mieko Mizutani,[1] Qing Nie,[2,3]
Frederic Y.M. Wan,[2,3] Yong-Tao Zhang,[2,3]
Peter Vilmos,[4,5] Rui Sousa-Neves,[4,5] Ethan Bier,[1,*]
J. Lawrence Marsh,[3,4,5] and Arthur D. Lander[3,4,5,*]
[1]Section of Cell and Developmental Biology
University of California, San Diego
La Jolla, California 92093
[2]Department of Mathematics
[3]Center for Complex Biological Systems
[4]Department of Developmental and Cell Biology
[5]Developmental Biology Center
University of California, Irvine
Irvine, California 92697

Summary

The dorsoventral axis of the *Drosophila* embryo is patterned by a gradient of bone morphogenetic protein (BMP) ligands. In a process requiring at least three additional extracellular proteins, a broad domain of weak signaling forms and then abruptly sharpens into a narrow dorsal midline peak. Using experimental and computational approaches, we investigate how the interactions of a multiprotein network create the unusual shape and dynamics of formation of this gradient. Starting from observations suggesting that receptor-mediated BMP degradation is an important driving force in gradient dynamics, we develop a general model that is capable of capturing both subtle aspects of gradient behavior and a level of robustness that agrees with in vivo results.

Introduction

Patterning of the dorsal-ventral axis of the *Drosophila* embryo is initiated by a nuclear gradient of the maternally deposited transcription factor Dorsal (Rusch and Levine, 1996), which activates expression of neuroectodermal genes such as *short gastrulation* (*sog*) (Francois et al., 1994; Markstein et al., 2002) in ventrolateral regions of the embryo, and nonneurectodermal genes such as *decapentaplegic* (*dpp*), *tolloid* (*tld*), and *twisted gastrulation* (*tsg*) in dorsal cells. By the midblastoderm stage, these zygotically active genes initiate a further round of patterning events, which lasts from the midcellular blastoderm stage through the beginning of gastrulation. During this time, the dorsal region of the embryo is subdivided into at least two distinct domains: an extraembryonic cell type known as amnioserosa (dorsal-most cells) and epidermal ectoderm (the ventral portion of the nonneural ectoderm). In the dorsal region, a variety of genes are expressed in nested patterns centered on the dorsal midline, in a process that reflects graded signaling by the bone morphogenetic protein (BMP) pathway (Ashe et al., 2000; Jazwinska et al., 1999; Ray et al., 1991; Wharton et al., 1993).

Activation of the BMP pathway in *Drosophila* embryos can be visualized directly, using immunohistochemistry to detect the phosphorylated form of the cytoplasmic protein Mad. Phosphorylated Mad (PMad) accumulates as a direct consequence of BMP receptor activation and translocates into the nucleus of responding cells (Dorfman and Shilo, 2001; Maduzia and Padgett, 1997; Raftery and Sutherland, 1999; Ross et al., 2001; Rushlow et al., 2001; Sutherland et al., 2003), where it acts as a transcriptional cofactor (Wotton and Massague, 2001). PMad is initially detected in a fairly broad and shallow pattern during midblastoderm stages, but then refines to a relatively sharp stripe of 5–7 cells at the dorsal midline (Dorfman and Shilo, 2001; Ross et al., 2001; Rushlow et al., 2001; Shimmi and O'Connor, 2003). Establishing this peak of PMad staining requires the function of at least four extracellular proteins besides Dpp itself: Sog (an antagonist of BMP signaling [Ferguson and Anderson, 1992; Francois et al., 1994; Yu et al., 1996]), Tsg (which binds to Sog and Dpp to form a trimeric inhibitory complex [Chang et al., 2001; Mason et al., 1994; Mason et al., 1997; Ross et al., 2001; Scott et al., 2001; Yu et al., 1996]), Tld (a protease that cleaves Sog [Marques et al., 1997; Shimell et al., 1991; Shimmi and O'Connor, 2003]), and Scw (another BMP ligand that increases the activity of Dpp [Arora et al., 1994; Nguyen et al., 1998]). The relationship between PMad staining and the expression of genes in broader dorsal patterns presumably reflects different threshold levels of BMP response (Ashe et al., 2000; Rushlow et al., 2001).

Ever since it became apparent that both Sog and Tsg can act as inhibitors of BMP activity, investigators have found it puzzling that loss of function of either of these molecules eliminates the peak of strong BMP signaling activity at the dorsal midline (Decotto and Ferguson, 2001; Harland, 2001; Holley et al., 1996; Ray and Wharton, 2001). How can antagonists be responsible for elevating the activity of the molecule they inhibit? To explain this seeming paradox, it has been suggested that Sog plays two roles in creating the BMP activity gradient. First, because it is present in a graded distribution—diffusing from lateral neural ectoderm to form a protein gradient in the dorsal ectoderm (Srinivasan et al., 2002)—Sog sets up a gradient of BMP inhibition from ventral to dorsal, limiting the ventral extent of BMP signaling. The view that Sog acts in this fashion is supported by the finding that domains of BMP target gene expression increase in width ventrally by several diameters in *sog*^{−/+} heterozygous embryos (Biehs et al., 1996) and expand to occupy most of the dorsal ectoderm in *sog* null embryos (Francois et al., 1994; Ray et al., 1991). Second, Sog has been proposed to bind BMPs and carry them dorsally, causing their accumulation at the dorsal midline (Holley et al., 1996). This role of Sog in BMP transport could then explain the greater levels of BMP signaling at the dorsal midline in wild-type versus *sog* null embryos (Ross et al., 2001; Rushlow et al., 2001). This ability of Sog to elevate BMP signaling at a distance from the site of Sog expression

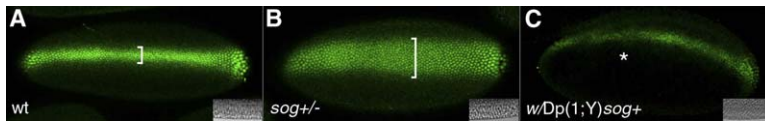*Correspondence: adlander@uci.edu (A.D.L.); ebier@ucsd.edu (E.B.)

Figure 1. The Distribution of PMad in Dorsal Cells Is Dependent on Sog Dosage

PMad staining in embryos at late blastoderm stage of the following genotypes: (A) wt (two copies of *sog*), (B) *sog*$^{-/+}$ (one copy of *sog*), and (C) *w*/Dp(1;Y)*sog*$^+$ (equivalent to four copies of *sog*). The dorsal PMad stripe spans 5–6 cells in wt embryos (A), whereas in the *sog*$^{-/+}$ embryo (B) it becomes twice as wide (10–13 cells). Conversely, an extra dosage of Sog leads to decreased levels of PMad and interruptions in the stripe (asterisk). Bars indicate the width of PMad expression and insets show Nomarski cross-sections of embryos that have completed cellularization. Mutant embryos in (B) and (C) were collected from *w* females crossed to *sog*^{6}/Dp(1;Y)*sog*$^+$ males carrying a duplication of *sog* on the Y chromosome. All resulting female embryos are *sog*$^{-/+}$ while male embryos are *w*/Dp(1:Y)*sog*$^+$. The two classes were unambiguously identified by double-labeling with an antibody against the female-specific Sex-lethal protein (not shown). For each of the genotypes shown, at least 20 embryos were examined. Within any given genotype, variability of only about 1–3 cells was observed in the widths of PMad stripes, i.e., a level much smaller than the observed differences between genotypes.

is also revealed by experiments in which Sog and Dpp are expressed at ectopic locations, studies that further demonstrate a requirement for Tld in this process (Ashe and Levine, 1999). Thus, the transport function of Sog has been viewed as a "shuttle," in which BMPs bind Sog, diffuse dorsally, and are then liberated in an active form by Sog cleavage (Ashe, 2002; Eldar et al., 2002; Meinhardt and Roth, 2002; Shimmi and O'Connor, 2003). In the case of Tsg, genetic and biochemical studies suggest that it is an essential cofactor in the binding of Dpp to Sog, thus participating in both the inhibitory activity of Sog as well as its transport function (Scott et al., 2001; Shimmi and O'Connor, 2003).

Given that crucial extracellular components involved in regulating BMP signaling in the early *Drosophila* embryo have been identified, and the time course of BMP activation can be followed by examination of PMad activation and expression of dosage-sensitive BMP target genes, this system is particularly amenable to quantitative analysis. Here we undertake such an analysis, beginning with a critical evaluation of several key properties (morphogen diffusibility, stability) and performance objectives (robustness) of the dorso-ventral patterning system. We provide experimental evidence that Dpp is readily diffusible in the embryo (whether or not Sog is present) and that patterning does not exhibit the high degree of robustness (lack of sensitivity to changes in *sog* dosage) that others have asserted (Eldar et al., 2002). We show that a relatively simple computational model, in which receptor-mediated morphogen degradation plays a central role, captures the Sog-dependent shuttling of BMPs to the midline and provides insights into the unusual dynamics of this gradient-forming process.

Results

The BMP Activity Gradient Is Not Robust with Respect to Changes in *sog* Gene Dosage

The fact that *Drosophila* embryos heterozygous for mutations in *sog*, *tsg*, *tld*, or *scw* develop into apparently normal adults (*dpp*, in contrast, is haploinsufficient [Irish and Gelbart, 1987]) suggests that the embryonic BMP signaling gradient is highly robust. However, several observations indicate otherwise. For example, expression of BMP target genes in the dorsal region of the embryo is sensitive to *sog* gene dosage (Biehs et al., 1996), and heterozygosity for *sog* can rescue the lethality caused by *dpp* haploinsufficiency (Francois et al., 1994) as well as that associated with a hypomorphic allele of *tld* (Ferguson and Anderson, 1992). The data in Figure 1 clearly show, in embryos of unambiguous

genotype, that changes in *sog* gene dosage have large effects on the dorsal PMad stripe at the final stage of blastoderm. In wild-type females, this stripe is ~5–6 cells across (Figure 1A), whereas in *sog*$^{-/+}$ females, it is approximately twice as wide (10–13 cells; Figure 1B). Conversely, when the *sog* dose is increased (two copies of *sog* in males or three in females), PMad staining is reduced in both breadth and intensity, with gaps at points along the midline (Figure 1C). These changes are sufficient to explain the ventrally expanded expression of BMP target genes in *sog*$^{-/+}$ heterozygous embryos (Biehs et al., 1996). The fact that *sog*$^{-/+}$ animals ultimately develop normally must therefore reflect regulation at later stages. Accordingly, marked robustness, at least with respect to *sog* dosage, is not a characteristic of the embryonic BMP gradient.

Dpp Acts at a Distance Even in the Absence of *sog*

BMPs are soluble in vitro, and previous studies on Dpp action in wing discs suggest unhindered BMP diffusion (Lander et al., 2002; Teleman and Cohen, 2000). This contrasts with the recent assertion that, to be able to form an appropriate gradient in the embryo, free BMPs must diffuse at least 100 times slower than BMPs that are in complex with Sog and/or Tsg (Eldar et al., 2002). We sought to investigate the in vivo diffusivity of BMPs in both the presence and absence of Sog. To do this, we expressed Dpp in various mutant backgrounds under the control of the *even-skipped* (*eve*) stripe 2 (st2) enhancer, and we measured ranges of gene induction and Mad phosphorylation relative to the endogenous 7-stripe *eve* expression pattern. Multilabeling in situ methods (Kosman et al., 2004) allowed us to compare multiple gene expression patterns within single, genotyped embryos.

In wild-type embryos with two copies of st2-*dpp*, the dorsal PMad stripe broadens to a maximum of 15–16 cells in the vicinity of st2, thinning back to its normal width posteriorly (Figures 2A and 2B). By the time the endogenous PMad stripe has refined (stage 6/7), the expansion of PMad activation extends back to between *eve*-stripes 5 and 6, a distance of ~25–30 cell diameters (Figure 2B). A similar effect on expression of *race* (a high-threshold *dpp* target gene) was observed in st2-*dpp* embryos (Figure 2D).

We then measured the effects of st2-*dpp* in a *sog*$^-$ mutant background. Since *race* expression is normally lost in most of the trunk and is maintained only in the region anterior to *eve*-st2 in *sog*$^-$ mutant embryos (Ashe and Levine, 1999; also compare Figures 2C and
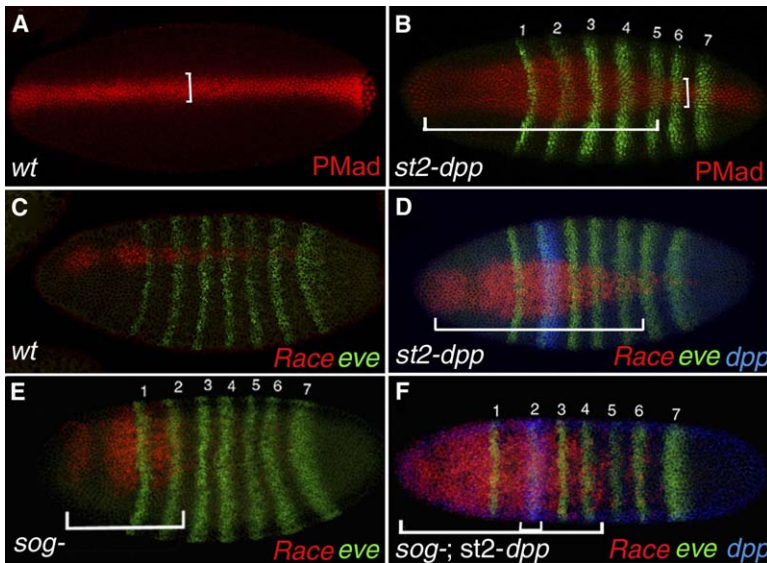
Figure 2. Dpp Acts at a Distance in the Absence of Sog

Dorsal view of blastoderm-stage embryos doubly stained for *eve* mRNA and either PMad (A and B) or *race* (C–F; in situ hybridization probes are indicated in the lower right corner of each figure). *eve* serves as a marker to measure distances along the AP axis between the st2 site of *dpp* expression and the range of ectopic PMad or *race* activation (indicated by the horizontal bars in [B], [D], and [F]).

(A) Dorsal PMad stripe in a wild-type (wt) embryo.

(B) *sog*⁺ embryo carrying two copies of st2-*dpp*. The PMad stripe in st2-*dpp* embryos assumes a bottle-like shape, which is broader nearest to the st2-*dpp*, tapering progressively further from the Dpp source, until regaining its normal width posterior to *eve*-st6 (compare vertical bars in [A] and [B]). Significant ectopic PMad activation extends to between *eve* stripes 5–6.

(C and D) A similar effect is observed on the Dpp target gene *race*, as shown. (C) Normal *race* pattern in a wt embryo, and (D) *race* expansion in a *sog*⁺; st2-*dpp* embryo also extends to *eve*-st6 (bracket).

(E and F) Dpp range of action was also measured in the absence of Sog by the ectopic activation of *race* by st2-*dpp*. In *sog*⁻ embryos, *race* expression is ordinarily restricted to the head (E, bar). Ectopic expression of st2-*dpp* in a *sog*⁻ background leads to a significant long distance activation of *race*, which extends to between *eve* stripes 4–5 (bars).

2E), any posterior *race* signal in *sog*⁻; st2-*dpp* embryos must come from the action of Dpp produced at st2. We find substantial posterior *race* expression in such embryos, extending to between *eve*-stripes 4 and 5 (Figure 2F). These results indicate that Dpp can act over 15–20 cell diameters in a *sog*⁻ background. A similar analysis of the range over which st2-*dpp* inhibits expression of the neural gene *ind* reveals effects over even greater distances (C.M. Mizutani et al., submitted).

Even when the spread of a morphogen is by diffusion, the range over which it acts will be set by the balance between diffusion and two other processes—production and removal (i.e., receptor-mediated uptake and degradation, as discussed in the next section). For example, no matter how slowly a molecule diffuses, one could achieve (in principle) as large a range of action as one liked simply by expressing it at high enough levels. To make sure that this effect did not account for the long range of Dpp action we observed in Figure 2, we examined individual st2-*dpp* embryos by in situ hybridization to compare *dpp* mRNA levels in *eve*-stripe 2 with those in the dorsal region of endogenous *dpp* expression outside of the st2-*dpp* domain. We found that, in embryos with two copies of st2-*dpp*, *dpp* expression within stripe 2 was only about 2.5- ± 0.7-fold higher than endogenous *dpp* expression. This difference would have had to be much larger to explain the range of action of st2-*dpp*, were Dpp only poorly diffusible (see Supplemental Data available with this article online).

We also examined the range of Dpp action in maternally lateralized embryos, which express no endogenous Dpp. In these embryos, *sog* is expressed globally throughout the neuralized ectoderm, and expression of a single copy of *eve* st2-*dpp* has no detectable effects (Figure 3A), presumably because Sog levels are high enough to fully antagonize BMP signaling. In contrast, when *sog* is removed from such embryos (i.e., in lateralized *sog*⁻; st2-*dpp* embryos), PMad staining is observed, which builds progressively to a domain 7–10 cells in either direction beyond the limits of eve2 expression (Figures 3B–3E). Thus, in a lateralized *sog*⁻ background, BMP activity also can spread a significant distance.

BMP Degradation and the Dynamics of Gradient Formation

In many morphogen systems, gradient formation is the direct result of a balance between morphogen production and morphogen degradation (Dubois et al., 2001; Eldar et al., 2003; Lander et al., 2002; Teleman and Cohen, 2000). Although little is known about BMP degradation in the *Drosophila* embryo, results in the larval wing disc argue that Dpp is rapidly turned over (Teleman and Cohen, 2000). Effects of receptor overexpression (Lecuit and Cohen, 1998) suggest that Dpp degradation in the disc is receptor driven (Lander et al., 2005), which is consistent with in vitro evidence that BMP binding triggers receptor-mediated endocytosis (Jortikka et al., 1997).

Although the embryonic BMP signaling gradient is much shorter lived (developing and acting over ~1 hr; Campos-Ortega and Hartenstein, 1985; Dorfman and Shilo, 2001) than its counterpart in the larval wing disc, we wondered whether BMP degradation might still play an important role in gradient formation. Measuring BMP degradation directly would be technically very difficult in the *Drosophila* embryo. Nevertheless, we can infer from experimental data that it must take place. For example, in Figure 3B, Dpp was expressed under the control of the *eve* st2 enhancer for a continuous period of about 45 min, in the absence of any Sog or endogenous Dpp. By fixing embryos at various times, we observed that levels of PMad staining evolved rapidly to a stable,
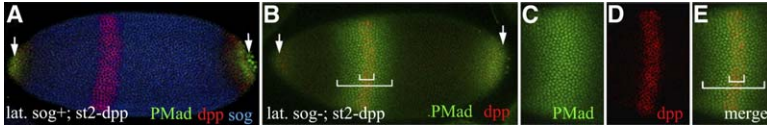
Figure 3. The Range of Action of Dpp in the Absence of Sog Was Assayed by PMad Expression in Lateralized Embryos with Uniform Levels of Dorsal

Mutant embryos were derived from sog^{U2} gd^7/ gd^7; Tl^3/+ crossed to st2-dpp males. In this case, endogenous dpp expression is absent and st2-dpp (one copy) is the only source of Dpp. In this lateralized background, sog is ubiquitously expressed (A), which in turn blocks Dpp activity in the vicinity of st2-dpp and results in no PMad staining except at the poles (arrows). Removal of sog (B–E) leads to ectopic activation of PMad in a stripe that is more than twice as wide as the st2-dpp stripe ([B], bars; [C]–[E] are higher-magnification views of the embryo in [B]).

unchanging pattern by about 30 min (data not shown). In the face of continuous Dpp production, if Dpp degradation were not occurring, PMad staining should continue to expand indefinitely outward from the Dpp source (Lander et al., 2002).

The fact that a steady pattern is reached within 30 min allows us to estimate the rate of Dpp degradation. This is because the system created by st2-dpp expression in a lateralized sog^- embryo matches a simple morphogen diffusion problem that we have previously analyzed (a stripe of morphogen production feeding a field of cells in which only diffusion and receptor-mediated binding and degradation take place [Lander et al., 2002; Lander et al., 2005]). To a first approximation, the approach to steady state of such a system is set by the time constant of degradation itself. Thus, a pattern that has reached two-thirds of its steady-state value by 35 min implies a degradation rate constant of at least 5×10^{-4} s^{-1}. This is in the same range as the rate constant for Dpp degradation in the wing disc, estimated as $\geq 2 \times 10^{-4}$ s^{-1} (Lander et al., 2002; Teleman and Cohen, 2000). Given the existence of a rapid degradative pathway, it makes little sense to ignore its potential influence on the establishment of the embryonic BMP gradient.

Creating a Dorsal Midline Peak Does Not Place Limits on BMP Diffusivity

The ability to create a sharp peak of morphogen activity at the dorsal midline is a remarkable feature of the embryonic BMP gradient. We wondered what roles robustness, BMP diffusivity, BMP degradation, and other phenomena played in the formation of such a peak. We therefore produced a simple computational model (Figure 4): within the geometry of the perivitelline space of the *Drosophila* embryo, Dpp, Sog, and Tsg are continuously produced in the appropriate places (the dorsal half of the embryo for Dpp and Tsg; the ventral half for Sog) at constant rates from a starting concentration of zero. Receptors are assumed to be at constant concentration everywhere and to continuously degrade bound BMPs. Dpp-Sog-Tsg complexes assemble and are then degraded at a constant rate by Tld to liberate free Dpp and Tsg. All secreted molecules are assumed to be freely diffusible, and Sog functions simply as a competitive inhibitor of Dpp binding to its receptor (another departure from the Eldar et al. [2002] model, which required Sog to displace Dpp from its receptors). We considered only a single BMP ligand (Dpp) rather than two independent ones (Dpp and Scw) for two reasons. First, our main goal was to identify the minimal conditions

that could reproduce the basic shapes and dynamics of the BMP gradient. Second, recent data suggest that the major signaling molecule in vivo is, in fact, a single ligand—a Dpp/Scw heterodimer—that interacts with Sog, Tsg, and Tld in the same ways as homodimeric Dpp, but with different affinities (Shimmi et al., 2005).

As shown in Figure 5, even this simple system can generate a sharp activity peak at the dorsal midline of the embryo in less than 30 min after the onset of Dpp production (also see Supplemental Data). Such a pattern agrees with the biological observation of a peak of Mad phosphorylation that quickly develops at about

$$\frac{\partial [L]}{\partial t} = D_L \frac{\partial^2 [L]}{\partial x^2} - k_{on}[L](R_0 - [LR]) + k_{off}[LR]$$
$$- j_{on}[L][ST] + (j_{off} + \tau)[LST] + V_L(x)$$

$$\frac{\partial [LR]}{\partial t} = k_{on}[L](R_0 - [LR]) - (k_{off} + k_{deg})[LR]$$

$$\frac{\partial [S]}{\partial t} = D_S \frac{\partial^2 [S]}{\partial x^2} - n_{on}[S][T] + n_{off}[ST] + V_S(x)$$

$$\frac{\partial [ST]}{\partial t} = D_{ST} \frac{\partial^2 [ST]}{\partial x^2} + n_{on}[S][T] - n_{off}[ST]$$
$$- j_{on}[L][ST] + j_{off}[LST]$$

$$\frac{\partial [T]}{\partial t} = D_T \frac{\partial^2 [T]}{\partial x^2} - n_{on}[S][T] + n_{off}[ST] + \tau[LST] + V_T(x)$$

$$\frac{\partial [LST]}{\partial t} = D_{LST} \frac{\partial^2 [LST]}{\partial x^2} + j_{on}[L][ST] - (j_{off} + \tau)[LST]$$

Figure 4. Partial Differential Equations Describing a "Minimal" Model of Gradient Formation Driven by Diffusion and Receptor-Mediated Ligand Degradation

L = BMP ligand (e.g., Dpp); R = receptor; S = Sog; T = Tsg; V_L, V_S, and V_T are production rates and D_L, D_S, and D_{ST}; D_T and D_{LST} are diffusion coefficients for their subscripted species; and association, dissociation, and degradation rate constants for L-R binding are represented by k_{on}, k_{off}, and k_{deg}, respectively. The assembly of LST complexes is modeled as initial S-T binding (with association and dissociation rate constants j_{on} and j_{off}) followed by L-ST binding (with association and dissociation rate constants of n_{on} and n_{off}), but analysis and calculations show that the output of the model is substantially the same for other assembly orders. In the absence of any data showing that free Sog and Tsg are degraded over the time course of embryonic patterning, these processes were generally not included (the effect of including degradation of free Sog [Srinivasan et al., 2002] was explored preliminarily, and unless very rapid, did not substantially influence the model's behavior). Tolloid-mediated cleavage of LST complexes was represented by a single first-order rate constant, τ.
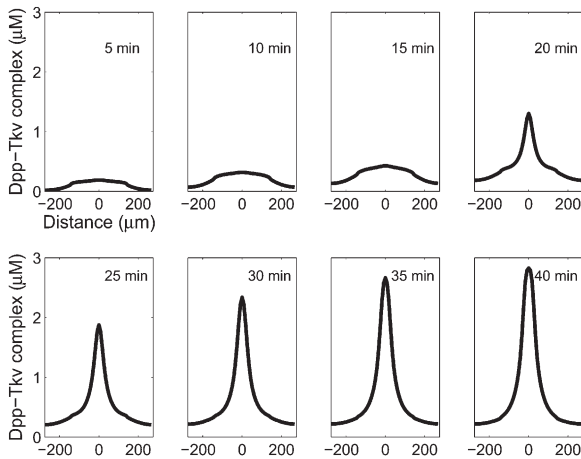
Figure 5. Time-Dependent Generation of a Peak of BMP Activity at the Dorsal Midline

For many parameter sets, an early phase with low level of BMP activity broadly distributed across the entire dorsal region is followed by the abrupt growth of a sharp midline peak. Parameters in this case were $D_L = D_S = D_{ST} = D_T = D_{LST} = 85$ μm^2 s^{-1}; $V_L = 1$ nM s^{-1} and limited to the dorsal region; $V_T = 4$ nM s^{-1} and limited to the dorsal region; $V_S = 80$ nM s^{-1} and limited to the ventral region; $k_{on} = 0.4$ μM^{-1} s^{-1}; $k_{off} = 4 \times 10^{-6}$ s^{-1}; $k_{deg} = 5 \times 10^{-4}$ s^{-1}; $j_{on} = 95$ μM^{-1} s^{-1}; $j_{off} = 4 \times 10^{-6}$ s^{-1}; $n_{on} = 4$ μM^{-1} s^{-1}; $n_{off} = 4 \times 10^{-5}$ s^{-1}; $\tau = 0.54$ s^{-1}; $R_0 = 3$ μM. The circumference of the embryo was taken to be 550 μm; with the dorsal midline set at $x = 0$, the dorsal half may be defined as $-137.5 < x < 137.5$ μm.

30 min and then stabilizes (Dorfman and Shilo, 2001; Sutherland et al., 2003). This behavior depends upon the presence of Sog and its cleavage by Tld. In the absence of Sog, the model predicts only a broad shallow peak of pMad activity (Figure 6A). The same picture

is seen in the absence of Tsg, whereas in the absence of Tld, BMP signaling is very low everywhere (Figure 6B). These predictions agree with in vivo observations (Mason et al., 1994; Ross et al., 2001; Shimmi and O'Connor, 2003; Yu et al., 2000) and support the view that a Sog/Tld-dependent BMP shuttling mechanism (Decotto and Ferguson, 2001; Holley et al., 1996; Ross et al., 2001; Shimmi and O'Connor, 2003) is responsible for the initial production of a midline peak of signaling. Apparently, such a mechanism can operate even if there is only one kind of BMP ligand and even if that ligand is freely diffusible, is produced continuously, and undergoes rapid receptor-mediated degradation.

The model also predicts—in agreement with the data in Figure 1—that the midline peak of BMP signaling will be significantly wider in $sog^{-/+}$ embryos and significantly narrower and lower in embryos with an extra dose of Sog (Figure 6A). Interestingly, the predicted increase in peak width in sog heterozygotes is not as large as that observed in vivo (Figure 1), even when looked at over a wide range of parameter values (see Discussion).

The dynamics of the growth of the midline PMad peak in the model are intriguing. As shown in Figure 5, no peak is seen for 15 min, then one abruptly rises over the next 5–10 min. The abrupt appearance of a midline peak matches in vivo observations, in which a midline stripe of strong PMad immunoreactivity appears rather suddenly between mid and late blastoderm stages (Ross et al., 2001, cf. Figures 1I and 1J; C.M.M. and E.B., unpublished observations), an interval corresponding to about 10 min (Campos-Ortega and Hartenstein, 1985).

Analysis of the model shows that the early "plateau phase" of relatively constant, low PMad staining reflects a time when the Sog and Dpp concentrations rise in parallel, leading to a relatively fixed level of free Dpp.
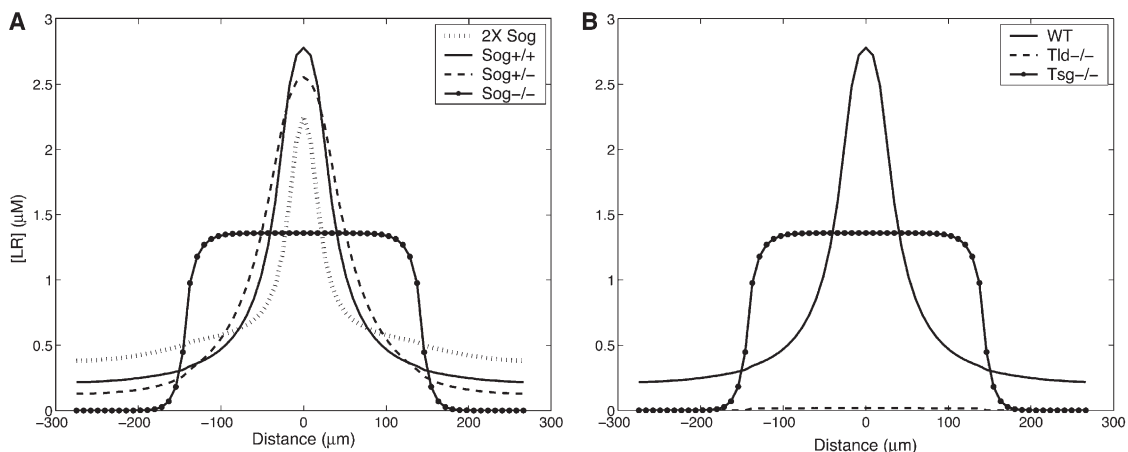

Figure 6. Calculated Effects of *sog*, *tld,* and *tsg* Mutations on the BMP Activity Gradient

Unless otherwise indicated, gradients were calculated using the parameters in Figure 5, and patterns shown are at 38 min after the onset of BMP production.

(A) Effects of *sog* gene dosage. The rate of Sog production was set to 0, 40, 80, or 160 nM s^{-1} to represent Sog$^{-/-}$, Sog$^{-/+}$, Sog$^{+/+}$, and 2× Sog animals, respectively. Increasing *sog* dosage generates a smaller, narrower peak, whereas decreasing *sog* dosage creates a broader peak (cf. Figure 1).

(B) Effect of *tld* and *tsg* mutations. In the absence of Tsg, a broad flat domain of BMP signaling is seen in the dorsal half of the embryo, similar to that in $sog^{-/-}$ mutants in (A). In the absence of Tld, BMP signaling is very low everywhere and exhibits no midline peak. These data are consistent with the dorsalized and ventralized phenotypes of $tsg^{-/-}$ and $tld^{-/-}$ mutants, respectively.
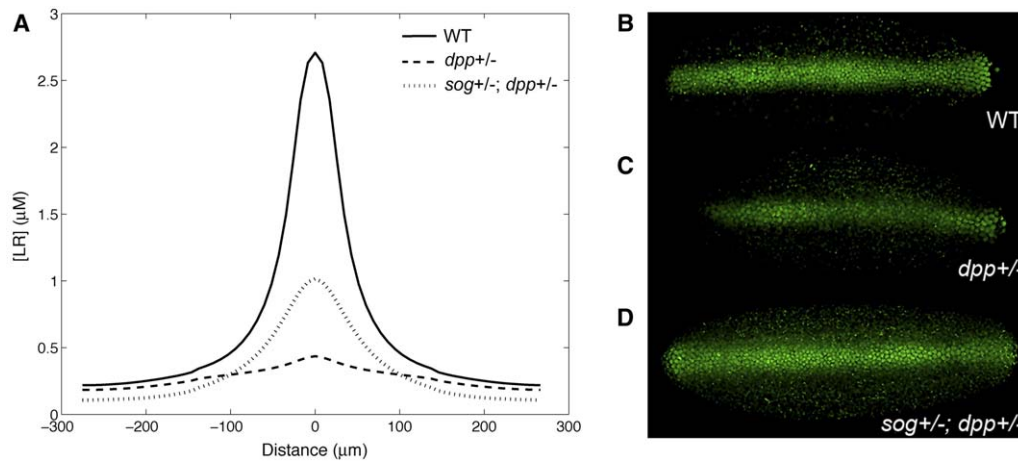
Figure 7. Reducing *sog* Gene Dosage Rescues Patterning Defects Caused by Reduced *dpp* Gene Dosage

(A) Predicted effects of decreasing the rate of BMP and Sog production on the formation of the embryonic BMP gradient. The highest and lowest curves show that halving BMP synthesis is expected to reduce the midline accumulation of BMP-receptor complexes markedly. The solid curve shows that additionally halving Sog production should be able to rescue, at least partially, the PMad distribution. Parameters were as in Figure 5. Patterns shown are at 36 min after onset of BMP production.

(B–D) PMad staining of wild-type (B), $dpp^{-/+}$ (C), and $sog^{-/+}$; $dpp^{-/+}$ (D) embryos (dorsal views). In a $dpp^{-/+}$ embryo (C), PMad staining is weaker and less regular than in wild-type. PMad staining in a $sog^{-/+}$; $dpp^{-/+}$ embryo (D) is stronger and more regular than in $dpp^{-/+}$ single mutants, although less regular than in wild-type embryos. Note also that the lateral expansion of PMad staining normally observed in $sog^{-/+}$ embryos (Figure 2B) is not seen in $sog^{-/+}$; $dpp^{-/+}$, indicating that *sog* and *dpp* exert opposing gene dosage effects that approximately cancel each other out in the double mutant condition. The embryos in (B)–(D) were stained in parallel, and the data were collected using the same confocal scanning settings. The embryos shown are representative of at least 20 embryos of each genotype. These results agree with earlier data showing that $dpp^{-/+}$ embryos exhibit a nearly complete loss of *race* expression posterior to *eve*-st2 (Rusch and Levine, 1997) and that $sog^{-/+}$; $dpp^{-/+}$ transheterozygotes exhibit a ~50-fold increase in viability when compared to $dpp^{-/+}$ embryos (Francois et al., 1994).

Over time, however, Dpp-dependent cleavage of Sog causes the release of bound Dpp, which binds to and causes the destruction of additional Sog, ultimately creating a chain reaction that leads to rapid loss of free Sog, and an abrupt jump in free and receptor bound Dpp. Interestingly, this dynamic behavior is not related to the ventrodorsal shuttling of BMPs. Even if all molecules were expressed everywhere in the embryo, one would still see this "plateau-jump" behavior, although it would occur everywhere at once, not just at the dorsal midline (see Supplemental Data).

A second interesting feature of the model is that it explains how reducing *sog* dosage can partially rescue the effects of reduced *dpp* dosage (Figure 7A). As mentioned earlier, embryos that are $dpp^{-/+}$ are substantially rescued from lethality by reduction in the dosage of *sog* (Francois et al., 1994). The data in Figures 7B–7D show that such rescue occurs at the level of the embryonic PMad pattern (rather than through some later compensatory process). These experimental results are surprising because, individually, *sog* and *dpp* mutations act in the same direction at the dorsal midline—they both lower the intensity of the PMad peak and decrease Dpp-dependent gene expression (Biehs et al., 1996; Rusch and Levine, 1996; Rusch and Levine, 1997). The model provides an explanation rooted entirely in the dynamics: *sog* and *dpp* mutations have opposite effects on the timing of the above-mentioned receptor occupancy jump. Thus, part of the decrease in PMad staining at the dorsal midline of a $dpp^{-/+}$ embryo is due to a delay in the onset of peak growth (i.e., the PMad peak is less far along at the time point examined). Reduction in *sog* dosage has the countervailing effect of accelerating peak growth (see Supplemental Data), compen-

sating, in the short term, for the effects of reduced *dpp* expression.

A third important feature of the model is that it predicts that Dpp's range of action should be greater in the presence of Sog than in its absence, even though Sog has no effect on the diffusion of Dpp. An example of this effect can be seen in the comparison of Figure 2D with 2F, which shows clearly that st2-Dpp acts at a greater distance in sog^+ than in sog^- embryos. It is easy to see how such data could lead one to conclude that Dpp diffuses faster in the presence of Sog (Eldar et al., 2002; Wang and Ferguson, 2005), but the model explains that such an inference (which is biochemically problematic, anyway) is not needed. The observed behavior can arise simply by virtue of the fact that Sog protects Dpp from receptor-mediated degradation, such degradation being rapid enough to keep its range of action otherwise fairly short. This range-enhancing effect of Sog is a generic one that any soluble inhibitor, at moderate concentrations, should have on a diffusible morphogen; it does not require Tld and is not the same as the shuttling mechanism that concentrates BMPs at the dorsal midline (see Supplemental Data). Clearly, there are multiple ways in which soluble inhibitors can redistribute morphogens, a point that may be of relevance in other morphogen systems where soluble inhibitors are expressed (e.g., Balemans and Van Hul, 2002; Kawano and Kypta, 2003).

Discussion

Dorsoventral patterning of the *Drosophila* ectoderm is driven by a morphogen gradient that is distinctive in at least three regards: it forms and acts quickly; it has an

unusual profile, with a sharp peak at the dorsal midline; and it relies upon the activities of at least three nonsignaling, secreted proteins (Sog, Tsg, and Tld). The goal of the present study was to reveal how these characteristics—dynamics, shape, and protein-protein interactions—depend on each other.

We began by showing that robustness with respect to variations in the expression of single genes is not a characteristic of this system (Figure 1). This is an important observation, given that considerable attention has been focused lately on the robustness of morphogen-patterning systems (Eldar et al., 2003; Houchmandzadeh et al., 2002; von Dassow et al., 2000), as well as biological signaling in general (Alon et al., 1999; Morohashi et al., 2002). The fact that $sog^{-/+}$ embryos eventually develop normally underscores the ability of embryos to compensate at later stages for early errors (cf. Houchmandzadeh et al., 2002). It is not clear why marked effects of *sog* heterozygosity were not seen in similar experiments by Eldar et al. (2002); this may have been related to their inability to genotype individual embryos, or to a lower sensitivity of PMad staining. We note that recent observations on accumulation of the co-smad Medea in wild-type and presumptive $sog^{-/+}$ embryos (Sutherland et al., 2003) look very similar to our observations on PMad in embryos of unambiguous genotype (Figures 1A and 1B).

We next examined the diffusibility of BMPs in the embryo in the presence and absence of Sog (Figures 2 and 3). Recently, Eldar et al. (2002) asserted that BMPs are effectively indiffusible in the embryo, except when complexed with Sog. In contrast, by examining embryos in which Dpp was ectopically expressed, we observed that the range of Dpp action was reduced in the absence of Sog, but still substantial, and consistent with unhindered diffusion. By observing the rate at which continuous ectopic Dpp expression gave rise to an unchanging response profile, we were also able to infer that Dpp must undergo rapid degradation, presumably through receptor-dependent means. In these experiments, levels of expression of ectopic Dpp were not high (2.5-fold above normal when two copies of st2-*dpp* were present, as in Figure 2; presumably only slightly above normal when one copy was present, as in Figure 3). It should also be noted that these results cannot be accounted for by the fact that Eve2 expression is weakly observed in a wider domain at its onset (Small et al., 1992), for several reasons. First, the rapidity with which early PMad signals are lost in the embryo (e.g., in lateral portions of the dorsal ectoderm) implies that there should be little perdurance of BMP signaling over the time course of the experiments in Figures 2 and 3. Second, the rapidity of Dpp degradation suggests that there should be little perdurance of Dpp-receptor complexes. Finally, it is clear that the range of Dpp action in Figure 2D extends more than two *eve* stripes past *eve*-st2 and continues to build progressively even after *eve*-st2 has fully refined to a narrow stripe.

We utilized the above observations to produce a simplified model of gradient formation. Our goal was not necessarily to reproduce all aspects of the in vivo gradient, but rather to begin with a minimum number of elements—and as few assumptions as possible—and then ask which of the behaviors of the in vivo gradient

could be captured. Interestingly, a great many of those behaviors emerge from a model in which a single ligand (e.g., Dpp or a Dpp/Scw heterodimer) diffuses freely, is degraded by receptors, forms a complex with Sog and Tsg, and is released from that complex when Tld cleaves Sog. These behaviors include rapid dynamics, formation of a broad domain of weak dorsal signaling that abruptly refines to a sharp midline peak, and peak narrowing or broadening when *sog* dosage is either increased or decreased, respectively (Figures 5 and 6). These behaviors depend upon the combined presence of Sog, Tsg, and Tld and are also highly sensitive to *dpp* dosage (in agreement with Dorfman and Shilo, 2001; Rusch and Levine, 1997; Sutherland et al., 2003). Interestingly, highly localized expression of Tld and an absolute dependence of Sog cleavage on Dpp are not essential (data not shown). Also not critical is the order of assembly of Dpp-Sog-Tld complexes.

Although the ability of the model to form a midline peak of BMP activity exemplifies the Sog/Tld-dependent "shuttling" proposed by others (Holley et al., 1996; Ross et al., 2001; Shimmi and O'Connor, 2003), that mechanism does not give a complete picture of events. For one thing, the abrupt onset of midline peak growth after a substantial plateau phase reflects a BMP-catalyzed chain reaction of Sog destruction that is independent of BMP transport per se. Second, calculations show that any soluble inhibitor has the ability to expand the range of action of a morphogen simply by protecting it from receptor-mediated destruction. Indeed, this effect alone could underlie some of the greater range of action of ectopically expressed Dpp in wild-type versus sog^- embryos.

At least one feature of the model that does not match in vivo observations, even when investigated over a wide range of parameter values, is the magnitude of the effect of *sog* heterozygosity on PMad peak width. Figure 1 suggests a near doubling of peak width, whereas calculations predict a more modest increase (Figure 6). Even accounting for the nonlinearity of immunohistochemistry and the fact that PMad may not be an instantaneous read-out of BMP receptor occupancy, the data suggest that other processes, not captured in the simple model, regulate the shape of PMad peaks. For example, it might be necessary to include the effects of a novel truncated form of Sog that promotes, rather than inhibits, BMP signaling (Yu et al., 2004).

One process that seems especially likely to shape PMad peaks is a BMP-driven, transcription-dependent feedback loop that has very recently been shown to markedly amplify high and depress low levels of BMP signaling in the *Drosophila* embryo (Wang and Ferguson, 2005). Such feedback could not only modify the shapes of PMad peaks, but also potentially explain another peculiarity of the model, which is that its peak heights and widths best fit mutant data when they are looked at up to the 30–45 min period, but not much later (i.e., not in the mathematical steady state). Since positive-feedback regulation of BMP signaling (Wang and Ferguson, 2005) can be expected to both sharpen and maintain patterns that might otherwise have continued to evolve, it is perhaps not surprising that, at long enough times, in vivo behavior diverges from predictions of the model. Put another way, this issue serves as a reminder that, unlike BMP gradients at lar-

val stages of *Drosophila* development (e.g., in the imaginal discs), the embryonic BMP gradient forms and acts so rapidly that there is little justification for assuming that steady-state calculations should reproduce in vivo observations. Indeed, it is only by considering the dynamics of gradient formation that the model presented here is able to explain the seemingly paradoxical result that decreased dorsal midline PMad staining in *dpp*⁻/⁺ embryos can be rescued by lowered *sog* dosage (Figure 7), when loss of *sog* function, by itself, is associated with decreased dorsal midline PMad staining.

In summary, the results presented here indicate that known properties of the molecules required for formation of the *Drosophila* embryonic BMP gradient are sufficient to account for many aspects of gradient dynamics, shape, and robustness, with no need for assumptions such as lack of diffusion of free BMP, transient BMP synthesis, removal of BMP from its receptors by Sog, or attainment of a steady state. Although computational data indicate that a Sog/Tld-dependent shuttling mechanism plays a key role in shaping and timing this BMP gradient, other dynamic processes appear to participate as well.

Experimental Procedures

Drosophila Stocks and Genetic Crosses

The following stocks were used: Canton-S and *w* (used as wild-type background), *sog*⁶/C(1)RM, *y w f*/Dp(1;Y)*y*⁺ *sog*⁺ *B*ˢ, *gd*⁷ *sog*^U2/FM7, *gd*⁷/FM7; *D*/TM3 *Sb, mwh[1] snk[1] red[1] e[1] Tl[3] ca[1]*/ TM3, *Sb*/Ms(3)R24, *y w*; st2-*dpp* (a gift from H. Ashe), and *w sog*^U2/FM7; st2-*dpp*. Description of mutations is found in Lindsley and Zimm (1992) and Flybase (http://flybase.bio.indiana.edu). Genotypes of *sog*⁻/⁺ heterozygote female and *w*/Dp(1;Y)*y*⁺ *sog*⁺ *B*ˢ male embryos resulting from the cross between *sog*⁶/Dp(1;Y)*y*⁺ *sog*⁺ *B*ˢ ˢ males and *w* females were determined by the expression of the Sex lethal, a female-specific protein. The same method was used to identify C(1)RM *y w*/Dp(1:Y) *y*⁺ *sog*⁺ *B*ˢ female embryos with extra copy of *sog*, collected from the *sog*⁶/C(1)RM, *y w f*/Dp(1;Y)*y*⁺ *sog*⁺ *B*ˢ stock. To create lateralized embryos with st2-*dpp* (Figure 3), *gd*⁷ *sog*^U2/*gd*⁷; *mwh[1] snk[1] red[1] e[1] Tl[3] ca[1]*/+ females were crossed to *yw*; st2-*dpp*/st2-*dpp* males. For scoring *sog*⁻ embryos in Figures 2E, 2F, and 3B, a *sog* in situ probe was used in addition to discriminate embryos that lack *sog* expression. Embryo collections were performed at 25°C.

For the analysis of *dpp* and *sog* gene dosage, we used the *dpp*^H46 *Sp*/CyO23, Df(2L) DTD48/CyO23, and *sog*⁶/Dp(1;Y) *y*+ *B*ˢ *sog*+ stocks. *dpp*⁻/⁺ heterozygotes were generated by crossing Df(2L)DTD48/CyO23 flies to *w*- and scoring the progeny for PMad staining, which fell into two clearly distinguishable classes: 3× *dpp*, very strong staining; and 1× *dpp*, weak staining. Double heterozygous *sog*⁻/⁺; *dpp*⁻/⁺ embryos were generated by crossing *dpp*^H46 *Sp*/CyO23 females to *sog*⁶/Dp(1;Y) *y*⁺ *B*ˢ *sog*⁺ males and screening female embryos expressing Sxl and scored for PMad staining. These embryos also fell into two clearly distinct categories: *sog*⁶/+; +/CyO23 (1× *sog*; 3× *dpp* = very strong and broad PMad staining) and the double heterozygotes, *sog*⁶/+; *dpp*^H46/+ (1× *sog*; 1× *dpp* = approximately wild-type level of PMad staining with some irregularity in pattern).

Immunofluorescence and In Situ Hybridization

A detailed description of fluorescent methods used to detect multiple RNA transcripts is given in Kosman et al. (2004). Probes were labeled with digoxigenin, biotin, fluorescein (Roche), and dinitrophenol (NEN) haptens. For double protein detection and in situ staining, fixed embryos were treated with acetone (10 min at −20°C) before hybridization to allow penetration of probes, as a substitute for proteinase K incubation (Nagaso et al., 2001). After this treatment, in situ hybridization was performed before immunostaining

with rabbit anti-phosphoMAD (1:2000, a gift from P. ten Dijke) and antibodies to detect the RNA-labeled probes. Detection of primary antibodies was performed either with secondary antibodies labeled with Alexa Fluor dyes (used at 1:500, Molecular Probes) or using the Zenon kit (Molecular Probes). For a list of primary and secondary antibodies used, see Kosman et al. (2004), and Supplemental Data. Detection of Sex lethal protein was done with M18 monoclonal antibody (used at 1:1000, Iowa Hybridoma Bank). Images of fluorescently labeled embryos were acquired on a Leica SP2-AOBS scanning confocal microscope with 20× and/or 40× objective lenses.

Intensity Measurement of Dpp RNA

Embryos carrying two copies of st2-*dpp* were labeled with a probe against Dpp RNA, and fluorescent signals were captured in a scanning Confocal series. Image stacks were analyzed using Leica software. Different "regions of interest" of equal area were selected in each of three areas of the embryo: within the st2-*dpp* stripe ventrally (1), outside of the st2-*dpp* stripe but within the dorsal ectoderm in which endogenous *dpp* is expressed (2), and in the ventral region of the embryo where no *dpp* is expressed (3, residual background of staining). Corrected intensity values for st2-*dpp* (1 minus 3) and endogenous *dpp* (2 minus 3) mRNA were computed and the ratio of st2-*dpp* and endogenous *dpp* intensities were calculated and averaged for five late blastoderm-stage embryos.

Computational Methods

Systems of equations were solved numerically using finite difference schemes. Diffusion terms were approximated by the second-order central difference, and temporal evolution was approximated by a fourth-order Adams-Moulton predictor-corrector method. The overall accuracy of the implementation is second-order in space and fourth-order in time.

Supplemental Data

Supplemental Data include 12 figures and Supplemental Experimental Procedures and can be found with this article online at http://www.developmentalcell.com/cgi/content/full/8/6/915/DC1/.

References

Alon, U., Surette, M.G., Barkai, N., and Leibler, S. (1999). Robustness in bacterial chemotaxis. Nature *397*, 168–171.

Arora, K., Levine, M.S., and O'Connor, M.B. (1994). The *screw* gene encodes a ubiquitously expressed member of the TGF-beta family required for specification of dorsal cell fates in the *Drosophila* embryo. Genes Dev. *8*, 2588–2601.

Ashe, H.L. (2002). BMP signalling: visualisation of the Sog protein gradient. Curr. Biol. *12*, R273–R275.

Ashe, H.L., and Levine, M. (1999). Local inhibition and long-range enhancement of Dpp signal transduction by Sog. Nature *398*, 427–431.

Ashe, H.L., Mannervik, M., and Levine, M. (2000). Dpp signaling thresholds in the dorsal ectoderm of the *Drosophila* embryo. Development *127*, 3305–3312.

Balemans, W., and Van Hul, W. (2002). Extracellular regulation of BMP signaling in vertebrates: a cocktail of modulators. Dev. Biol. *250*, 231–250.

Biehs, B., Francois, V., and Bier, E. (1996). The *Drosophila short gastrulation* gene prevents Dpp from autoactivating and suppressing neurogenesis in the neuroectoderm. Genes Dev. *10*, 2922–2934.

Campos-Ortega, J.A., and Hartenstein, V. (1985). The Embryonic Development of *Drosophila melanogaster*, First Edition (Berlin: Springer Verlag).

Chang, C., Holtzman, D.A., Chau, S., Chickering, T., Woolf, E.A., Holmgren, L.M., Bodorova, J., Gearing, D.P., Holmes, W.E., and Brivanlou, A.H. (2001). Twisted gastrulation can function as a BMP antagonist. Nature *410*, 483–487.

Decotto, E., and Ferguson, E.L. (2001). A positive role for Short gastrulation in modulating BMP signaling during dorsoventral patterning in the *Drosophila* embryo. Development *128*, 3831–3841.

Dorfman, R., and Shilo, B.Z. (2001). Biphasic activation of the BMP pathway patterns the *Drosophila* embryonic dorsal region. Development *128*, 965–972.

Dubois, L., Lecourtois, M., Alexandre, C., Hirst, E., and Vincent, J.P. (2001). Regulated endocytic routing modulates wingless signaling in *Drosophila* embryos. Cell *105*, 613–624.

Eldar, A., Dorfman, R., Weiss, D., Ashe, H., Shilo, B.Z., and Barkai, N. (2002). Robustness of the BMP morphogen gradient in *Drosophila* embryonic patterning. Nature *419*, 304–308.

Eldar, A., Rosin, D., Shilo, B.Z., and Barkai, N. (2003). Self-enhanced ligand degradation underlies robustness of morphogen gradients. Dev. Cell *5*, 635–646.

Ferguson, E.L., and Anderson, K.V. (1992). Localized enhancement and repression of the activity of the TGF-beta family member, decapentaplegic, is necessary for dorsal-ventral pattern formation in the *Drosophila* embryo. Development *114*, 583–597.

Francois, V., Solloway, M., O'Neill, J.W., Emery, J., and Bier, E. (1994). Dorsal-ventral patterning of the *Drosophila* embryo depends on a putative negative growth factor encoded by the *short gastrulation* gene. Genes Dev. *8*, 2602–2616.

Harland, R.M. (2001). Developmental biology. A twist on embryonic signalling. Nature *410*, 423–424.

Holley, S.A., Neul, J.L., Attisano, L., Wrana, J.L., Sasai, Y., O'Connor, M.B., De Robertis, E.M., and Ferguson, E.L. (1996). The *Xenopus* dorsalizing factor noggin ventralizes *Drosophila* embryos by preventing DPP from activating its receptor. Cell *86*, 607–617.

Houchmandzadeh, B., Wieschaus, E., and Leibler, S. (2002). Establishment of developmental precision and proportions in the early *Drosophila* embryo. Nature *415*, 798–802.

Irish, V.F., and Gelbart, W.M. (1987). The decapentaplegic gene is required for dorsal-ventral patterning of the *Drosophila* embryo. Genes Dev. *1*, 868–879.

Jazwinska, A., Rushlow, C., and Roth, S. (1999). The role of brinker in mediating the graded response to Dpp in early *Drosophila* embryos. Development *126*, 3323–3334.

Jortikka, L., Laitinen, M., Lindholm, T.S., and Marttinen, A. (1997). Internalization and intracellular processing of bone morphogenetic protein (BMP) in rat skeletal muscle myoblasts (L6). Cell. Signal. *9*, 47–51.

Kawano, Y., and Kypta, R. (2003). Secreted antagonists of the Wnt signalling pathway. J. Cell Sci. *116*, 2627–2634.

Kosman, D., Mizutani, C.M., Lemons, D., Cox, W.G., McGinnis, W., and Bier, E. (2004). Multiplex detection of RNA expression in *Drosophila* embryos. Science *305*, 846.

Lander, A.D., Nie, Q., and Wan, F.Y. (2002). Do morphogen gradients arise by diffusion? Dev. Cell *2*, 785–796.

Lander, A.D., Nie, Q., and Wan, F.Y.M. (2005). Spatially distributed morphogen synthesis and morphogen gradient formation. Math. Biosci. Eng. *2*, 239–262.

Lecuit, T., and Cohen, S.M. (1998). Dpp receptor levels contribute to shaping the Dpp morphogen gradient in the *Drosophila* wing imaginal disc. Development *125*, 4901–4907.

Lindsley, D.L., and Zimm, G.G. (1992). The Genome of *Drosophila melanogaster*, First edition (San Diego: Academic Press).

Maduzia, L.L., and Padgett, R.W. (1997). *Drosophila* MAD, a member of the Smad family, translocates to the nucleus upon stimulation of the dpp pathway. Biochem. Biophys. Res. Commun. *238*, 595–598.

Markstein, M., Markstein, P., Markstein, V., and Levine, M.S. (2002). Genome-wide analysis of clustered Dorsal binding sites identifies putative target genes in the *Drosophila* embryo. Proc. Natl. Acad. Sci. USA *99*, 763–768.

Marques, G., Musacchio, M., Shimell, M.J., Wunnenberg-Stapleton, K., Cho, K.W., and O'Connor, M.B. (1997). Production of a DPP activity gradient in the early *Drosophila* embryo through the opposing actions of the SOG and TLD proteins. Cell *91*, 417–426.

Mason, E.D., Konrad, K.D., Webb, C.D., and Marsh, J.L. (1994). Dorsal midline fate in *Drosophila* embryos requires *twisted gastrulation*, a gene encoding a secreted protein related to human connective tissue growth factor. Genes Dev. *8*, 1489–1501.

Mason, E.D., Williams, S., Grotendorst, G.R., and Marsh, J.L. (1997). Combinatorial signaling by Twisted Gastrulation and Decapentaplegic. Mech. Dev. *64*, 61–75.

Meinhardt, H., and Roth, S. (2002). Developmental biology: sharp peaks from shallow sources. Nature *419*, 261–262.

Morohashi, M., Winn, A.E., Borisuk, M.T., Bolouri, H., Doyle, J., and Kitano, H. (2002). Robustness as a measure of plausibility in models of biochemical networks. J. Theor. Biol. *216*, 19–30.

Nagaso, H., Murata, T., Day, N., and Yokoyama, K.K. (2001). Simultaneous detection of RNA and protein by in situ hybridization and immunological staining. J. Histochem. Cytochem. *49*, 1177–1182.

Nguyen, M., Park, S., Marques, G., and Arora, K. (1998). Interpretation of a BMP activity gradient in *Drosophila* embryos depends on synergistic signaling by two type I receptors, SAX and TKV. Cell *95*, 495–506.

Raftery, L.A., and Sutherland, D.J. (1999). TGF-beta family signal transduction in *Drosophila* development: from Mad to Smads. Dev. Biol. *210*, 251–268.

Ray, R.P., and Wharton, K.A. (2001). Twisted perspective: new insights into extracellular modulation of BMP signaling during development. Cell *104*, 801–804.

Ray, R.P., Arora, K., Nusslein-Volhard, C., and Gelbart, W.M. (1991). The control of cell fate along the dorsal-ventral axis of the *Drosophila* embryo. Development *113*, 35–54.

Ross, J.J., Shimmi, O., Vilmos, P., Petryk, A., Kim, H., Gaudenz, K., Hermanson, S., Ekker, S.C., O'Connor, M.B., and Marsh, J.L. (2001). Twisted gastrulation is a conserved extracellular BMP antagonist. Nature *410*, 479–483.

Rusch, J., and Levine, M. (1996). Threshold responses to the dorsal regulatory gradient and the subdivision of primary tissue territories in the *Drosophila* embryo. Curr. Opin. Genet. Dev. *6*, 416–423.

Rusch, J., and Levine, M. (1997). Regulation of a dpp target gene in the *Drosophila* embryo. Development *124*, 303–311.

Rushlow, C., Colosimo, P.F., Lin, M.C., Xu, M., and Kirov, N. (2001). Transcriptional regulation of the *Drosophila* gene zen by competing Smad and Brinker inputs. Genes Dev. *15*, 340–351.

Scott, I.C., Blitz, I.L., Pappano, W.N., Maas, S.A., Cho, K.W., and Greenspan, D.S. (2001). Homologues of Twisted gastrulation are extracellular cofactors in antagonism of BMP signalling. Nature *410*, 475–478.

Shimell, M.J., Ferguson, E.L., Childs, S.R., and O'Connor, M.B. (1991). The *Drosophila* dorsal-ventral patterning gene tolloid is related to human bone morphogenetic protein 1. Cell *67*, 469–481.

Shimmi, O., and O'Connor, M.B. (2003). Physical properties of Tld, Sog, Tsg and Dpp protein interactions are predicted to help create a sharp boundary in Bmp signals during dorsoventral patterning of the *Drosophila* embryo. Development *130*, 4673–4682.

Shimmi, O., Umulis, D., Othmer, H., and O'Connor, M. (2005). Facilitated transport of a Dpp/Scw heterodimer by Sog/Tsg patterns the dorsal surface of the *Drosophila* blastoderm embryo. Cell *120*, 873–886.

Small, S., Blair, A., and Levine, M. (1992). Regulation of even-skipped stripe 2 in the *Drosophila* embryo. EMBO J. *11*, 4047–4057.

Srinivasan, S., Rashka, K.E., and Bier, E. (2002). Creation of a Sog morphogen gradient in the *Drosophila* embryo. Dev. Cell *2*, 91–101.

Sutherland, D.J., Li, M., Liu, X.Q., Stefancsik, R., and Raftery, L.A. (2003). Stepwise formation of a SMAD activity gradient during dorsal-ventral patterning of the *Drosophila* embryo. Development *130*, 5705–5716.

Teleman, A.A., and Cohen, S.M. (2000). Dpp gradient formation in the *Drosophila* wing imaginal disc. Cell *103*, 971–980.

von Dassow, G., Meir, E., Munro, E.M., and Odell, G.M. (2000). The segment polarity network is a robust developmental module. Nature *406*, 188–192.

Wang, Y.-C., and Ferguson, E.L. (2005). Spatial bistability of Dpp-receptor interactions during *Drosophila* dorsal-ventral patterning. Nature *434*, 229–234.

Wharton, K.A., Ray, R.P., and Gelbart, W.M. (1993). An activity gradient of decapentaplegic is necessary for the specification of dorsal pattern elements in the *Drosophila* embryo. Development *117*, 807–822.

Wotton, D., and Massague, J. (2001). Smad transcriptional co-repressors in TGF beta family signaling. Curr. Top. Microbiol. Immunol. *254*, 145–164.

Yu, K., Sturtevant, M.A., Biehs, B., Francois, V., Padgett, R.W., Blackman, R.K., and Bier, E. (1996). The *Drosophila decapentaplegic* and *short gastrulation* genes function antagonistically during adult wing vein development. Development *122*, 4033–4044.

Yu, K., Srinivasan, S., Shimmi, O., Biehs, B., Rashka, K.E., Kimelman, D., O'Connor, M.B., and Bier, E. (2000). Processing of the *Drosophila* Sog protein creates a novel BMP inhibitory activity. Development *127*, 2143–2154.

Yu, K., Kang, K.-W., Heine, P., Pyati, U., Srinivasan, S., Biehs, B., Kimelman, D., and Bier, E. (2004). Cysteine repeat domains and adjacent sequences determine distinct BMP modulatory activities of the *Drosophila* Sog protein. Genetics *166*, 1323–1336.